Intersubunit allosteric communication mediated by a conserved loop in the MCM helicase

Intersubunit allosteric communication mediated by a conserved loop in the MCM helicase

Elizabeth R. Barry[a,b], Janet E. Lovett[c], Alessandro Costa[b], Susan M. Lea[b], and Stephen D. Bell[b,1]

[a]MRC Cancer Cell Unit, Hutchison MRC Centre, Hills Road, Cambridge CB2 0XZ, United Kingdom; [b]Sir William Dunn School of Pathology, South Parks Road, Oxford OX2 6NA, United Kingdom; and [c]Centre for Advanced ESR, Inorganic Chemistry Laboratory, South Parks Road, Oxford OX1 3QR, United Kingdom

Edited by Charles C. Richardson, Harvard Medical School, Boston, MA, and approved December 5, 2008 (received for review September 17, 2008)

The minichromosome maintenance (MCM) helicase is the presumptive replicative helicase in archaea and eukaryotes. The archaeal homomultimeric MCM has a two-tier structure. One tier contains the AAA+ motor domains of the proteins, and these are the minimal functional helicase domains. The second tier is formed by the N-terminal domains. These domains are not essential for MCM helicase activity but act to enhance the processivity of the helicase. We reveal that a conserved loop facilitates communication between processivity and motor tiers. Interestingly, this allostery seems to be mediated by interactions between, rather than within, individual protomers in the MCM ring.

archaea | DNA replication | AAA+ protein | *Sulfolobus*

The two most highly studied archaeal minichromosome maintenance helicases (MCMs) are from *Methanothermobacter thermautotrophicus* (Mth) and *Sulfolobus solfataricus* (Sso) (1). Electron microscopy of full-length MthMCM in conjunction with X-ray crystallographic studies of the N-terminal domains of that protein has revealed that MthMCM is based on a heptameric or hexameric assembly in which the C-terminal motor domains form a ring that is stacked on a second ring formed by the N-terminal domains (2–4). Studies of SsoMCM have revealed that the hexameric form of the molecule interacts with DNA substrates (5). A central hole passes through the hexamer, and residues found within the pore are important for DNA binding (2, 5). More specifically, each monomer contributes a β-hairpin in the N terminus that extends into the central channel. Mutation of conserved basic residues at the tip of the hairpin impairs but does not abrogate DNA binding and helicase activities of the full-length SsoMCM protein. A second β-hairpin has also been identified in the AAA+ motor domain of the protein (5). Importantly, mutation of a conserved lysine in this hairpin only modestly reduces DNA binding by MCM but abolishes helicase activity, suggesting that this feature of the protein is involved in the "power stroke" of the helicase motor. Interestingly, mutation of either N or C-terminal β-hairpin residues has only modest effects on the basal ATPase activity of the helicase (measured in the absence of DNA). However, for both mutants, the addition of DNA did not result in the stimulation of ATPase activity detected with the wild-type protein (5). In agreement with the nonessential nature of the N-terminal β-hairpin for helicase activity, we have shown that it is possible to delete the N-terminal domains of SsoMCM entirely and still retain helicase activity of the C-terminal, AAA+ containing, half of the protein (C-half) or even just the isolated AAA+ domain (6). Addition of protein corresponding to the N-terminal domains modulated the range of substrates that could be melted by, and enhance the processivity of, the AAA+ domain construct. The processivity enhancement depended on the ability of the N-terminal β-hairpin to interact with DNA, suggesting that the N-terminal domains do not simply form a circular collar on which the AAA+ domains sit, but may in fact play a more dynamic role. The means of communication between N- and C-terminal tiers of the protein is not yet understood. A recent study has found that mutation of a conserved loop that extends from the main body of the N-terminal tier severely impairs the helicase activity of MthMCM, leading to speculation that this loop may be an important contact point between the two tiers (7). In this article, we describe a series of experiments that address the functional basis of the role of this conserved loop in SsoMCM. We find that deletion of the loop abrogates the helicase activity of MCM and reduces ATPase activity but does not significantly alter DNA binding by the helicase. However, deletion of the loop enhances the interaction between N- and C-terminal halves of MCM in a nucleotide-independent manner, revealing that the loop is not simply a static binding site for MCM. Importantly, helicase activity can be restored to a loop-deleted mutant by a second site deletion of the N-terminal β-hairpins, suggesting that the loop is involved in transducing positional cues to this motif. We additionally investigate whether the loop is acting to mediate communication within a single protomer or between adjacent protomers in the MCM ring. A combination of cross-linking analyses and EPR spectroscopy reveals that the loop plays a role in intersubunit allosteric communication. For this reason, we will refer to the loop in the following as the ACL (allosteric communication loop).

Results

The N-Terminal Tier of MCM Is Required for Localized Cooperativity. We have performed a series of mutant-doping experiments to investigate the manner in which ATP usage is coupled to helicase activity in SsoMCM (8). Our data revealed that SsoMCM helicase activity has an unusual mode of ATP usage where localized cooperativity exists between pairs of subunits within the hexameric assembly. This contrasts with the probabilistic hydrolysis mechanism seen with the ClpX AAA+ protease (9) or the sequential model determined for DnaB-type DNA helicases (10). We have demonstrated that the N-terminal domains of SsoMCM are dispensable for helicase activity. However, truncations lacking the N-terminal domains have modified properties, including relaxed substrate specificity and reduced processivity (6). We therefore tested the importance of the N-terminal domains of SsoMCM for the paired cooperativity behavior. Accordingly, we prepared proteins corresponding to residues 267–686 of either wild-type MCM (C-half) or a derivative containing a K $\rightarrow$ A mutation of the conserved Walker A lysine residue (K346 in the full-length protein). Our previous work (8) has shown that doping full-length Walker A mutant into helicase assays containing wild-type protein results in a nonlinear decrease in activity following the red curve in Fig. 1*A* and *G*. The nonlinearity of the doping response is indicative of cooperativity. In contrast, when we performed assays with our

Author contributions: E.R.B., J.E.L., A.C., and S.D.B. designed research; E.R.B., J.E.L., and A.C. performed research; E.R.B., J.E.L., A.C., S.M.L., and S.D.B. analyzed data; and E.R.B. and S.D.B. wrote the paper.

The authors declare no conflict of interest.

This article is a PNAS Direct Submission.

[1]To whom correspondence should be addressed. E-mail: stephen.bell@path.ox.ac.uk.

This article contains supporting information online at www.pnas.org/cgi/content/full/0809192106/DCSupplemental.

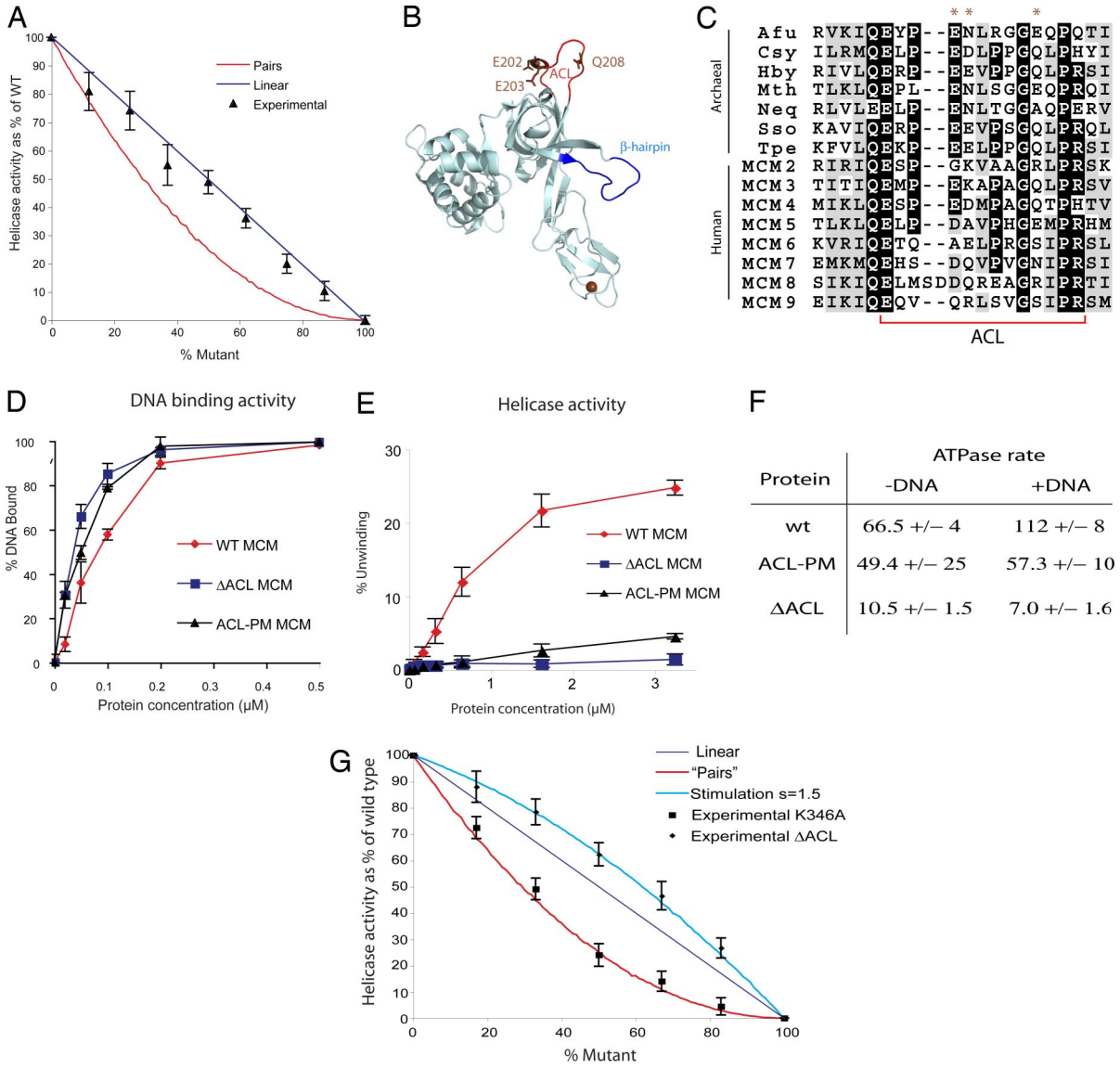

Fig. 1. A conserved loop in the N-terminal tier of MCM is required for intersubunit communication. (*A*) Mutant doping assay using the C-half of both wild-type MCM (residues 267–612) and Walker A lysine–alanine mutant (K346A in the full-length protein) in varying proportions in helicase assays. The red line indicates the nonlinear behavior of the full-length proteins (ref. 8). (*B*) Structure of the N-terminal 265 residues of SsoMCM [Protein Data Bank (PDB) ID code 2vl6]. The figure was by using PyMOL (http://pymol.sourceforge.net). The ACL is highlighted in red, and residues E202, E203, and Q208 are shown in brown stick form. The N-terminal DNA-binding β-hairpin is shown in dark blue. A zinc ion is shown as a brown sphere. (*C*) Sequence line-up of the ACL of seven representative archaeal MCM sequences (Afu, *Archaeoglogus fulgidus*; Csy, *Cenarchaeum symbiosum*; Hby, *Hyperthermus butylicus*; Mth, *M. thermautotrophicus*; Neq, *Nanoarchaeum equitans*, Sso, *S. solfataricus*; Tpe, *Thermofilum pendens*) together with human MCM2–9. The ACL is indicated in red, and residues corresponding to SsoMCM E202, E203, and Q208 are indicated by brown asterisks. (*D*) DNA binding to a flayed duplex substrate for wild-type MCM (WT-MCM), ΔACL, and ACL-PM (E202A, E203A, and Q207A) are shown (analogous results for ssDNA and dsDNA are shown in Fig S2). Error bars in this and all other panels are ±SD. (*E*) DNA helicase activity of WT, ΔACL, and ACL-PM MCM. (*F*) ATPase rates of the WT, ΔACL, and ACL-PM MCM. Values are picomoles of ATP hydrolyzed per second per nanomole of MCM (as monomer). (*G*) Mutant doping with ΔACL or Walker A mutant (K346A) into wild-type MCM. The helicase activities of the protein mixtures were measured and plotted relative to the activity of wild-type protein. Simulations (red and cyan lines) were performed as described in ref. 8.

truncated C-half proteins, we observed a linear decrease of activity as we increase the proportion of Walker A mutant protein (Fig. 1*A*). A linear response could be indicative of either a lack of cooperativity between subunits or, more trivially, of an inability of mutant and wild-type to interact with one another upon mixing. We performed pulldown experiments to test this latter possibility and found that wild-type and Walker A mutant C-half proteins are equally capable of homo- and heteromultimerization [supporting information (SI) Fig. S1]. Taken together, these data indicate that the N-terminal domains are required for mediating cooperativity between ATPase active sites within the MCM ring.

Basic Properties of ACL Mutant Proteins. Examination of the X-ray crystal structures of the N-terminal domains of MCM reveals the presence of a conserved loop (ACL) that faces the position that is believed to be occupied by the C-terminal motor domains of the protein (2, 18). To test the importance of the ACL for MCM activity, we have made two mutant derivatives (Fig. S2). In the first, which we named ACL-PM (ACL point mutant), we mutated residues E202, E203, and Q208 (in brown in Fig. 1 *B* and *C*) to alanines; and in the second, which we named ΔACL, we replaced the loop residues E199–R211 (in red and brown in Fig. 1 *B* and *C*) with the tripeptide serine–asparagine–glyine. The

resultant proteins were purified by heat treatment of the *Escherichia coli* extract, followed by centrifugation to remove precipitated protein. This was followed by chromatography on a heparin column and gel filtration on a Superdex 200 column. The MCMs were heat-stable and eluted as hexamers on gel filtration chromatography, indicating that the mutations had not grossly perturbed the protein structure (Fig. S3). In agreement with this, we found that both proteins had slightly higher (maximally 2-fold) DNA binding affinities compared with wild-type protein (Fig. 1*D* and Fig. S3). However, the ACL-PM had severely impaired DNA helicase activity, whereas the ΔACL mutant had no detectable helicase activity even at high protein concentrations (Fig. 1*E*). ACL-PM showed lower ATPase activity than wild type, and the ATPase activity was stimulated to a lesser extent by DNA. The ATPase activity of ΔACL was severely reduced and showed no DNA stimulation (Fig. 1*F*).

Because the ACL-PM shows a phenotype intermediate between wild type and ΔACL, we have focused on the ΔACL mutant in the subsequent experiments because this mutant seems to represent complete loss of function of this region. We next performed mutant-doping experiments with the ΔACL protein (Fig. 1*G*). To eliminate the possibility that the different DNA-binding affinities of the wild-type and mutant proteins (half-maximal binding at ≈100 and 50 nM protein, respectively; Fig. 1*D*) could influence these assays, we performed these experiments at 1 μM protein. The inhibition profile of this mutant is reminiscent of that seen with analogous experiments with a Sensor 1 N448E mutation (8). Using our described Monte Carlo-based simulations, we can account for this behavior by imposing the three simple rules: a pair of wild-type subunits has normal activity, a WT–mutant pair has a modestly (1.5-fold) enhanced activity, but a pair of mutant subunits has no activity. These data therefore implicate the ACL in mediating the localized cooperativity between pairs of protomers within the MCM hexamer. To test the possibility that ACL residues might contribute directly to the ATPase active site, we attempted to complement *cis* and *trans* mutants (*cis* mutants, such as altered Walker A or Sensor 1 residues, are defective in the ATPase-binding site of a given subunit; *trans* residues, such as the arginine finger, communicate with the active site of their neighbor). We have demonstrated that mixing of *cis* and *trans* mutants restores helicase activity (8); however, the ΔACL could not complement either class of mutant, indicating a distinct role (Fig. S4).

ACL and Interdomain Communication. Studies of the ACL of MthMCM led to the suggestion that the ACL might be a key interface between the N-terminal and C-terminal tiers of MCM (7). However, it has not been possible to test this hypothesis because the isolated C-terminal domain of MthMCM is insoluble. In contrast, however, the analogous fragment of SsoMCM is soluble and active in helicase assays. This allows us to test whether the ACL might be involved in interaction between the two tiers. We have described pulldown assays that reveal that the isolated N terminus of SsoMCM (residues 1–266, hereafter called N-half) can interact with a matrix coated with the immobilized C-terminal half of the protein (6). Using this assay, we observe that deletion of the ACL does not reduce binding of the N-half to the C-half but, rather, significantly enhances it (Fig. 2*A*). This enhancement is not affected by the presence of various adenine nucleotides in the binding buffer (Fig. S5). We have shown that addition of the wild-type N-half stimulates the helicase activity of the AAA+ domain of the protein on flayed duplex DNA substrates (6). In contrast, as can be seen in Fig. 2*B*, addition of the ACL-deleted N-half significantly reduces the helicase activity of the AAA+ domain, in agreement with the abrogation of the helicase activity of full-length ACL-deleted MCM. Thus, the ACL deletion does not prevent interaction between the N-and C-terminal halves of MCM.

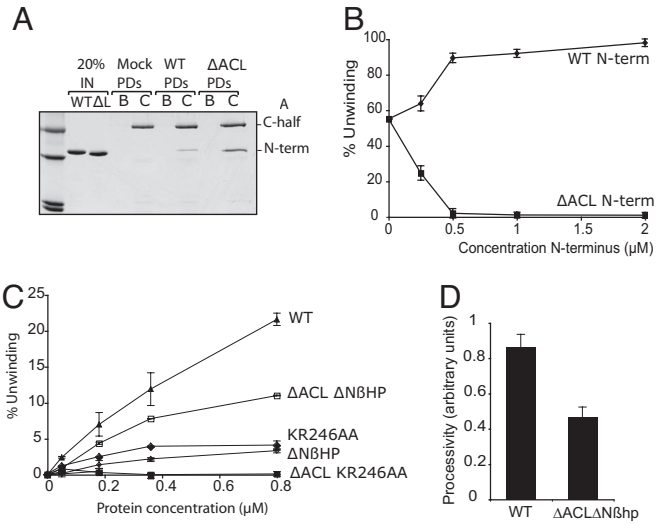

Fig. 2. Functional consequences of ACL deletion. (*A*) Pulldown assays of wild-type (WT) or ΔACL versions of the N-terminal domains of MCM (residues 1–266) on a matrix with immobilized C-half of MCM. After pulldown and washing, proteins were eluted by boiling in SDS/PAGE loading buffer. Proteins were detected after SDS/PAGE by staining with Coomassie brilliant blue. The positions of the various species are indicated. Analogous assays performed in the presence of ADP, ATP, AMP-PNP, and ADP-AlFx are shown in Fig. S5. (*B*) Helicase assays mediated by 0.5 μM C-half of MCM supplemented with increasing amounts of either wild-type or ΔACL N-half. (*C*) Helicase assays with full-length proteins with either wild-type, deleted (ΔNβHP) or point-mutated (KR246AA) N-terminal β-hairpin proteins with additional deletion of the ACL (ΔACL) as indicated. (*D*) Comparison of the relative processivity of wild-type or ΔNβHPΔACL proteins.

Interplay Between the ACL and the N-Terminal β-Hairpin. We have shown that the isolated C-half, and even the isolated AAA+ domain alone, retains helicase activity (ref. 6 and see above). Thus, the N-terminal domains are not essential for helicase activity. Paradoxically, however, our data reveal that deletion of the ACL abrogates helicase activity. We have shown that the addition of the N-terminal domains clearly elevates the activity and enhances the processivity of the AAA+ domain and that this depends on the ability of the N-terminal β-hairpins to interact with DNA (6). We speculated that the ACL may function by transducing a signal from the AAA+ domain to the N-terminal β-hairpin. Accordingly, we deleted the N-terminal β-hairpin by replacing residues I239–S249 (in dark blue in Fig. 1*A*) with a serine–asparagine–glycine tripeptide (ΔNβhp). This affected the multimeric status of the protein; gel filtration analyses revealed that the predominant peak of elution for ΔNβhp and ΔACL/ΔNβhp proteins was in agreement with these species existing as a mixture of dimers and monomer (Fig. S6). This is similar to what is seen for isolated N-half, C-half, and AAA+ domain MCM. When this mutation was introduced in the context of the wild-type protein (ΔNβhp) the resulting protein retained very low levels of helicase activity, similar to, but slightly lower than, that seen for the K246A/R247A mutant [in which conserved basic residues at the tip of the hairpin have been mutated to alanine (5)]. In contrast, when the N-terminal β-hairpin was removed we observed restoration of helicase activity with this double mutant protein (Fig. 2*C*). However, although this functioned well as a helicase on flayed duplex oligonucleotide substrates with 44 bp of dsDNA, in agreement with our previous data on the processivity of the isolated AAA+ domain, it showed much lower processivity than the wild-type protein (Fig. 2*D* and Fig. S7). The same restoration was not seen for the ΔACL K246A/R247A mutant, where residues at the tip of the N-terminal β-hairpin are mutated, but the hairpin itself is

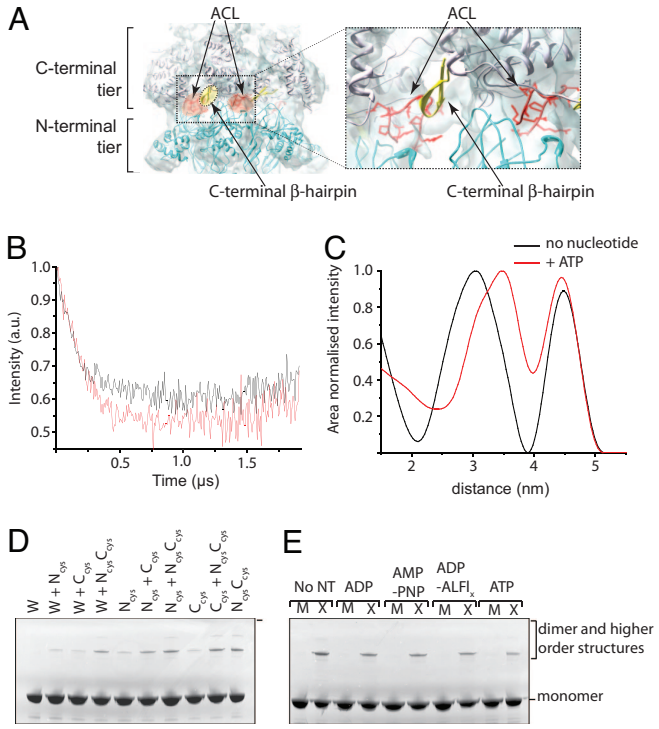

Fig. 3. Nucleotide-modifiable communication between the C-terminal pre-Sensor 1 β-hairpin and the ACL. (*A*) (*Left*) Superposition of the MthMCM EM structure (4) with the known structure of MthMCM N-terminal domains (in cyan; the ACL is highlighted in red). The C-terminal domains are modeled based on the structure of a bacterial ATPase (PDB ID code 2R44) that is predicted to have secondary structure architecture similar to MCM (conserved domain database expected value = $1\times e^{-4}$). (*Right*) Enlargement of the selected area. The C-terminal β-hairpin is highlighted in yellow. (*B*) DEER time trace after background correction shown in black for nucleotide-free MCM and in red MCM in the presence of 10 mM ATP. The best-fit line was found by using a Tikhonov regularization parameter of 1,000 and is shown in red. (*C*) The distance distributions corresponding to the DEER traces shown in *B*; black is nucleotide-free MCM, and red is MCM in the presence of 10 mM ATP. (*D*) Results of cross-linking assays with S206C (Ncys), K430C (Csys) single mutants or S206CK430C (NcysCsys) double mutants. The positions of monomer, dimer, and higher-order species are indicated. Wild-type (cysteine-free protein) is labeled W. M refers to mock-treated (reaction minus BMOE), and X indicates reactions treated with BMOE. (*E*) Cross-linking assays performed between S206C (Ncys) and K430C (Ccys) in the presence or absence of the indicated nucleotide (at 10 mM).

still present (Fig. 2*C*). We interpret these data as indicating that, in the absence of the ACL, the N-terminal β-hairpin is mispositioned in the central cavity of the helicase and may thereby inhibit helicase activity.

The ACL Mediates Intersubunit Communication. We have shown that a candidate β-hairpin in the AAA+ domain of SsoMCM is essential for the helicase activity of MCM (5). An analogous hairpin in SF3 helicases undergoes a large conformational alteration during the cycle of ATP binding, hydrolysis, and release (11, 12). Interestingly, mutation of this hairpin results in an MCM that can still bind DNA but has no helicase activity and no longer shows DNA-mediated stimulation of its ATPase activity. Because these behaviors are similar to that observed with the ACL-deleted mutation, we speculated that the ACL might communicate with the C-terminal β-hairpin. This proposal is supported by modeling based on the EM structure of MthMCM. As can be seen in Fig. 3*A*, the ACL lies in the vicinity of the C-terminal β-hairpin of the modeled position of a related AAA+ domain. However, it is not clear from the model whether this would be an intra- or intersubunit interaction. If this is an intrasubunit interaction, the ACL and C-terminal β-hairpin will be <5 Å distant from one another; if, in contrast, they mediate intersubunit interactions, then the ACL and C-terminal β-hairpin of a given subunit will be ≈30 Å apart. Thus, we sought to measure the distance between the ACL and C-terminal β-hairpin of a given subunit by using EPR spectroscopy.

To this end, we prepared mutant MCM that had cysteine substitutions at S206 of the ACL and the K430 of the C-terminal β-hairpin. [These experiments were performed with modified MCMs in which the 2 accessible cysteines at the C terminus of the proteins were mutated to serine; these alterations do not lead to any detectable modification of MCM activities (5)]. The Cys residues at the ACL and C-terminal β-hairpin were conjugated to nitroxide spin labels generating double-labeled protomers. Next, we mixed the labeled subunits with an 8-fold excess of wild-type MCM (without C-terminal cysteines) so that the majority of hexamers would only contain one labeled subunit. Analyzing these molecules by double electron electron resonance (DEER) we found that the closest distance between these residues was 29.5 ± 4 Å (black traces in Fig. 3 *B* and *C*). We additionally observe a second distance peak with a maximum at 45 Å; however, the $\tau 2$ for the pulse sequence configuration is not enough to measure this distance dependably. This second peak may represent the distance between the spin labels when the multiple-labeled MCM protomers are assembled into a single hexamer. Because the above data were derived in the absence of supplemental nucleotide, we repeated the experiment in the presence of ATP (red traces in Fig. 3 *B* and *C*) and found a significant lengthening of the ACL–C-terminal β-hairpin distance to 34.5 ± 4Å, indicative of ATP-induced conformational alterations in the relative positions of ACL and C-terminal β-hairpin within a subunit.

The ≈30 Å distance between ACL and C-terminal β-hairpin suggests that these residues lay on opposite faces of the MCM monomer. In accordance with the model in Fig. 3*A*, we speculated that the ACL of one subunit may be in the vicinity of the C-terminal β-hairpin of its neighbor. To test this hypothesis, we used the S206C and/or C-terminal β-hairpin residue K430C MCM mutants. We then tested the ability of the homobifunctional sulfydryl-specific cross-linker bismaleimidoethane (BMOE) to cross-link between these residues. Significantly, we could detect cross-linking between distinct monomers that possessed S206C (Ncys) and K430C (Ccys) (Fig. 3*D*). In contrast, homohexamers containing either of these mutations individually showed significantly reduced cross-linking. Because the BMOE has a spacer arm of just 8 Å, this indicates very close apposition of the C-terminal β-hairpin of one subunit with the ACL of a neighboring protomer. Significantly, the degree of cross-linking observed varied depending on the presence of nucleotide in the buffer. More specifically, cross-linking was highest in the absence of nucleotide and lowest in the presence of ATP (Fig. 3*E*). This indicates that the relative positioning of the ACL of one protomer and the C-terminal β-hairpin of its neighbor changes depending on the nucleotide status of the AAA+ domain.

Discussion

Our data provide a mechanistic basis for the previous observation that the ACL is important for MCM helicase activity (7) by revealing that this conserved motif is required for allosteric communication between subunits within the MCM hexamer. Our data indicate that the N-terminal domains of MCM and the C-terminal AAA+ domains can still interact in the absence of the ACL and do so in a manner that is independent of the presence of nucleotide. This indicates that there is an as yet unidentified constitutive interface between the N- and C-terminal tiers of MCM. This may be conceptually analogous to the IGF loops that mediate tight contact between ClpP and ClpX in the bacterial ClpPX proteolytic AAA+ machine (13–15).

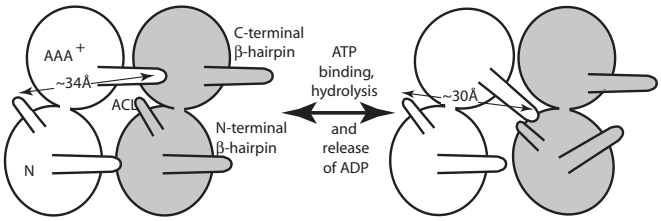

Fig. 4. Model for the interplay between C-terminal β-hairpin of one subunit and the ACL of its neighboring subunit in modulation of the position of the neighbor's N-terminal β-hairpin. We propose that, during the cycle of ATP binding and hydrolysis and release of ADP from one subunit, its C-terminal β-hairpin is repositioned, allowing it to contact the ACL of its neighbor and thus reposition the N-terminal β-hairpin of that subunit. (*Left*) The 34-Å distance indicated in the white subunit would correspond to the ATP-bound version of the protein. (*Right*) The 30-Å distance between the white subunit ACL and C-terminal β-hairpin and close apposition of the β-hairpin to the ACL of the neighboring subunit would correspond to the nucleotide-free form.

Although our data reveal that the ACL is not required for interaction between the N-terminal and AAA+ tiers of the protein, our EPR and cross-linking data indicate that the ACL of one protomer is in close proximity to the C-terminal β-hairpin within the AAA+ domain of another protomer in the MCM hexamer. Furthermore, the relative positioning of these two features is modulated by the presence of nucleotide. By analogy with other AAA+ proteins, and in agreement with the observed behavior of MCM with mutations in this hairpin (5, 11, 12), it is likely that the position of the hairpin will alter during the ATPase cycle of the subunit. Thus, an individual β-hairpin will differentially contact the ACL of the neighboring subunit during ATPase cycle, thereby communicating conformational alterations in the AAA+ domain of one subunit to the N-terminal domains of another (Fig. 4). Our observation that the effect of the ACL deletion can be alleviated by deletion of the N-terminal β-hairpin suggests that, in the absence of the ACL, the N-terminal β-hairpin is locked in an inhibitory configuration. We propose, therefore, that the ACL acts to modulate the positioning of the N-terminal β-hairpin in tune with the ATP cycle of the AAA+ motor domain of the neighboring subunit (Fig. 4). Here again, parallels can be drawn with the ClpP–ClpX interaction. The pore 2 loop in ClpX has been shown to contact the "N-terminal loop" in ClpP, and furthermore, this interaction is modulated by the presence of nucleotide (15). This analogy is strengthened by the fact that both the ClpX pore 2 loop and MCM C-terminal β-hairpin are located between the Walker B and Sensor 1 elements of the AAA+ domain. Thus, as with ClpP–ClpX, we observe two forms of interaction between N-terminal and AAA+ domain-containing tiers of MCM: a static, nucleotide-independent interface and a dynamic, nucleotide-modifiable interaction. That these similarities exist between divergent AAA+ proteins suggests a generalized model for inter-tier communication within AAA+ machines irrespective of whether the two tiers are composed of covalently contiguous subunits, as in MCM, or by two separate rings, as in ClpP–ClpX.

Methods

Additional procedures are discussed in *SI Methods*.

Cloning, Mutagenesis, and Protein Purification. All constructs used were described (5, 6). Point mutagenesis was performed as described in ref. 8. Loop deletion (ACL and N-terminal β-hairpin) and replacement with the SNG tripeptide were achieved by PCR amplification around the pET30a-MCM/N-half plasmid by using primers that annealed at either end of the loop, one of which included an overhang encoding the SNG tripeptide. All proteins were expressed and purified as described (5, 6), except that for full-length MCM mutants with mutations in the N-terminal β-hairpin (K246A/R247A ΔACL, ΔNβhp, ΔNβhp ΔACL) an additional HiTrap Q column purification step was performed between heparin and gel filtration (Fig. S2). For the corresponding N-terminal domain constructs, the heparin purification step was omitted because the proteins did not bind to heparin.

Gel Filtration Analysis. Gel filtration analysis was performed on a Superdex 200 10/300 gel filtration column (GE Healthcare), in 20 mM Tris (pH 8), 150 mM NaCl, and 1 mM DTT, with 100 μL of 50 μM protein. This was run at 0.5 mL/min. The amplitudes of the resulting peaks were normalized by using the UNICORN program.

ATPase, Helicase, EMSA, and Pulldown Interaction Assays. ATPase assays were performed essentially as described in ref. 5 except that 275 μM ATP was used, and reactions were performed for 30 min at 60 °C. Helicase and EMSA assays were performed on Y-shaped substrates, ssDNA, or dsDNA as described (5, 6), except that for full-length MCM (and mutants) helicase assays were performed at 65 °C, whereas for C-half and AAA+ core constructs (and mutants) helicase assays were performed at 50 °C. For further details see *SI Methods*. All results shown are the result of at least three independent repeats. Error bars represent 1 SEM. Pulldown interaction assays were performed as described in ref. 6.

Cross-Linking. Proteins were mixed to give a final concentration of 5 μM in 1× PBS (pH 7), 5 mM EDTA (with nucleotide at 10 mM if applicable) in a 50-μL reaction volume. Bis(maleimido)ethane (Pierce) was added to give a final concentration of 100 nM. Cross-linking was quenched after 2 min by boiling in SDS/PAGE loading buffer [1.05% (wt/vol) SDS, 62.5 mM Tris·HCl (pH 6.8), 10% (vol/vol) glycerol, 0.35 M 2-mercaptoethanol, 0.0125% (wt/vol) bromophenol blue). Twenty microliters was resolved by SDS/PAGE.

EPR. Proteins were derivatized with (1-oxyl-2,2,5,5-tetramethyl-D3-pyrroline-3-methyl)methanethiosulfonate (Toronto Research Chemicals). Spin-labeled protein (25 μM) was mixed with wild-type protein a final total protein concentration of 200 μM. The spin-labeled protein solution had 30% glycerol added, and 50 μL was put in a 3-mm outer diameter quartz tube. The sample was then frozen in liquid nitrogen and inserted into a 3-mm split ring EPR resonator (Bruker). Using a Bruker ELEXSYS 680 EPR spectrometer operating at X-band (≈9.3 GHz) the four-pulse DEER experiments were performed at 50 K (16). The sequence in the observer frequency was $\pi/2$-τ1-π-τ2-π-τ2-echo with 32-ns pulse lengths. The second, pump, frequency was set at the maximum of the nitroxide spectrum that was offset by −65 MHz from the observer frequency. The pump pulse consisted of a single π pulse of 12-ns duration and was inserted between the two π pulses of the observer frequency with time (τ1+τ2+t) where τ was incremented by 8 ns each time. A +/− phase cycle was applied to the first observer pulse, and proton modulations were minimized by varying τ1 from 200 ns to 264 ns in eight steps. The τ2 delay was 2 μs, and each trace had 255 points, 13 scans were taken, there experiment was repeated with three independent samples. Data processing was carried out with DeerAnalysis2006 and Tikhonov regularization and the L-curve method for estimating the correct regularization parameter (17).

Modeling. EM structure visualization and atomic coordinate fitting were performed by using Chimera.

ACKNOWLEDGMENTS. We thank Silvia Onesti for supplying the EM map used in Fig. 3*A*. S.D.B.'s laboratory is supported by the Edward Penley Abraham Trust and the Medical Research Council. J.E.L. and S.M.L. are funded by Engineering and Physical Sciences Research Council and the University of Oxford.

1. Costa A, Onesti S (2008) The MCM complex: (Just) a replicative helicase? *Biochem Soc Trans* 36:136–140.
2. Fletcher RJ, *et al.* (2003) The structure and function of MCM from archaeal *M. thermoautotrophicum*. *Nat Struct Biol* 10:160–167.
3. Pape T, *et al.* (2003) Hexameric ring structure of the full-length archaeal MCM protein complex. *EMBO Rep* 4:1079–1083.
4. Costa A, *et al.* (2006) Structural basis of the *Methanothermobacter thermautotrophicus* MCM helicase activity. *Nucleic Acids Res* 34:5829–5838.
5. McGeoch AT, Trakselis MA, Laskey RA, Bell SD (2005) Organization of the archaeal MCM complex on DNA and implications for the helicase mechanism. *Nat Struct Mol Biol* 12:756–762.
6. Barry ER, McGeoch AT, Kelman Z, Bell SD (2007) Archaeal MCM has separable processivity, substrate choice, and helicase domains. *Nucleic Acids Res* 35:988–998.
7. Sakakibara N, *et al.* (2008) Coupling of DNA binding and helicase activity is mediated by a conserved loop in the MCM protein. *Nucleic Acids Res* 36:1309–1320.

8. Moreau MJ, McGeoch AT, Lowe AR, Itzhaki LS, Bell SD (2007) ATPase site architecture and helicase mechanism of an archaeal MCM. *Mol Cell* 28:304–314.
9. Martin A, Baker TA, Sauer RT (2005) Rebuilt AAA+ motors reveal operating principles for ATP-fuelled machines. *Nature* 437:1115–1120.
10. Crampton DJ, Mukherjee S, Richardson CC (2006) DNA-induced switch from independent to sequential dTTP hydrolysis in the bacteriophage T7 DNA helicase. *Mol Cell* 21:165–174.
11. Gai DH, Zhao R, Li DW, Finkielstein CV, Chen XS (2004) Mechanisms of conformational change for a replicative hexameric helicase of SV40 large tumor antigen. *Cell* 119:47–60.
12. Enemark EJ, Joshua-Tor L (2006) Mechanism of DNA translocation in a replicative hexameric helicase. *Nature* 442:270–275.
13. Kim YI, Burton RE, Burton BM, Sauer RT, Baker TA (2000) Dynamics of substrate denaturation and translocation by the ClpXP degradation machine. *Mol Cell* 5:639–648.
14. Singh SK, *et al.* (2001) *J Biol Chem* 276:29420–29429.
15. Martin A, Baker TA, Sauer RT (2007) Distinct static and dynamic interactions control ATPase–peptidase communication in a AAA+ protease. *Mol Cell* 27:41–52.
16. Pannier M, Veit S, Godt A, Jeschke G, Spiess HW (2000) Dead-time free measurement of dipole–dipole interactions between electron spins. *J Magn Reson* 142:331–340.
17. Jeschke G, *et al.* (2006) DeerAnalysis2006: A comprehensive software package for analyzing pulsed ELDOR data. *App Magn Reson* 30:473–498.
18. Liu W, *et al*. (2008) Structural analysis of the *Sulfolobus solfataricus* MCM protein N-terminal domain. *Nucleic Acids Res* 36:3235–3243.